Alkanethiolate-Protected PbS Nanoclusters: Synthesis, Spectroscopic and Electrochemical Studies

Shaowei Chen,* Lindsay A. Truax, and Jennifer M. Sommers

Department of Chemistry, Southern Illinois University, Carbondale, Illinois 62901-4409

Received August 16, 2000. Revised Manuscript Received October 6, 2000

A series of alkanethiolate-passivated PbS nanoparticles were synthesized with varied feed ratios of the starting reactants, lead acetate and alkanethiols, and characterized by using a variety of spectroscopic and electrochemical techniques. Transmission electron microscopic studies revealed that, of all the samples prepared, the particle size mainly fell into the range of 2–4 nm in diameter, with mostly spherical shape and modest dispersity. In addition, the particles were found to be quite stable where the particle size varied only slightly during particle growth. UV–Vis spectroscopy showed an absorption edge at a wavelength between 700 and 800 nm for the larger particles (>3 nm in diameter), while for the smaller particles (2.5 nm in diameter), the absorption edge was found at 560 nm, which was consistent with the size-dependent quantum confinement effect of PbS nanoparticles. Photoluminescence studies were carried out by measuring the excitation and emission spectra of the PbS nanoparticles in solutions, where the fluorescence was found at around 804 nm and the peak intensity appeared to be depressed greatly by the presence of transition-metal (e.g., Au, Ag, and Pd) nanoparticles, despite the relatively weak absorption of metal particles at the red end. Electrochemical studies of the PbS nanoparticles in solution revealed an analogue to the Coulomb blockade that arose from the particle band gap structure within the potential range of from −0.8 to +0.8 V, and at potentials beyond this range, cathodic reduction as well as anodic dissolution of PbS resulted in a series of voltammetric waves, where rather significant overpotentials were observed as compared to those in aqueous media.

Introduction

The recent intense research interests in nanosized particles of metals and semiconductors have been mainly attributed to the so-called quantum size effect, i.e., the size-tunable materials properties. For semiconductor nanoparticles, this is distinctly reflected in the rather significant band gap structure that is size-sensitive, and might be manifested by the varied luminescence characteristics.[1-13] Of these, lead sulfide (PbS) is a unique semiconductor material, with a rather small band gap (0.41 eV at 300 K); this band gap can be easily manipulated by the material's dimensions, reaching a few electronvolts when PbS particles in the nanometer regime are formed.[3,8] Thus, a great deal of research effort has been devoted to the method development for the synthesis of PbS particles of varied sizes in a controllable manner. Among these, the most common routes involve using strong matrix supports to stabilize the particles, including organic[3,7,8] and inorganic (e.g., glass and ceramic)[9] polymers, where the particles are embedded in the supporting media forming nanocomposite structures. Another approach entails using inverse micelle[10] or microemulsion[11] systems as the nanoreactors and as the protecting media. In addition, semiconductor nanoparticles have been generated by using amphiphilic monolayers at the air/water

* To whom all correspondence should be addressed (E-mail: schen@chem.siu.edu).

(1) Henglein, A. *Chem. Rev.* **1989,** *89,* 1861 and references therein.

(2) (a) Steigerwald, M. L.; Brus, L. E. *Acc. Chem. Res.* **1990,** *23,* 183. (b) Nirmal, M.; Brus, L. *Acc. Chem. Res.* **1999,** *32,* 407. (c) Empedocles, S.; Bawendi, M. G. *Acc. Chem. Res.* **1999,** *32,* 389.

(3) (a) Wang, Y. *Acc. Chem. Res.* **1991,** *24,* 133. (b) Wang, Y.; Herron, N. *J. Phys. Chem.* **1991,** *95,* 525. (c) Wang, Y.; Suna, A.; Mahler, W.; Kasowski, R. *J. Chem. Phys.* **1987,** *87,* 7315.

(4) Weller, H. *Adv. Mater.* **1993,** *5,* 88.

(5) (a) Alivisatos, A. P. *J. Phys. Chem.* **1996,** *100,* 13226. (b) Peng, X.; Wickham, J.; Alivisatos, A. P. *J. Am. Chem. Soc.* **1998,** *120,* 5343. (c) Bruchez, M., Jr.; Moronne, M.; Gin, P.; Weiss, S.; Alivisatos, A. P. *Science* **1998,** *281,* 2013. (d) Chan, W. C. W.; Nie, S. *Science* **1998,** *281,* 2016.

(6) (a) Zhang, J. Z. *Acc. Chem. Res.* **1997,** *30,* 423. (b) Zhang, J. Z. *J. Phys. Chem. B* **2000,** *104,* 7239.

(7) Möller, M.; Spatz, J. P. *Curr. Opin. Colloid Interface Sci.* **1997,** *2,* 177.

(8) (a) Kane, S. R.; Cohen, R. E.; Silbey, R. *Chem. Mater.* **1996,** *8,* 1919. (b) Kane, S. R.; Cohen, R. E.; Silbey, R. *J. Phys. Chem.* **1996,** *100,* 7928.

(9) (a) Borrelli, N. F.; Smith, D. W. *J. Non-Cryst. Solids* **1994,** *180,* 25. (b) Martucci, A.; Innocenzi, P.; Fick, J.; Mackenzie, J. D. *Non-Cryst. Solids* **1999,** *244,* 55. (c) Salata, O. V.; Dobson, P. J.; Hull, P. J.; Hutchison, J. L. *Adv. Mater.* **1994,** *6,* 772. (d) Parvathy, N. N.; Pajonk, G. M.; Rao, A. V. *J. Cryst. Growth* **1997,** *179,* 249.

(10) (a) Fendler, J. H. *Chem. Rev.* **1987,** *87,* 877. (b) Liveri, V. T.; Rossi, M.; D'Arrigo, G.; Manno, D.; Micocci, G. *Appl. Phys. A* **1999,** *69,* 369.

(11) Yang, J. P.; Qadri, S. B.; Ratna, B. R. *J. Phys. Chem.* **1996,** *100,* 17255.

(12) (a) Meldrum, F. C.; Flath, J.; Knoll, W. *Langmuir* **1997,** *13,* 2033. (b) Li, L. S.; Qu, L.; Wang, L.; Lu, R.; Peng, X.; Zhao, Y.; Li, T. *J. Langmuir* **1997,** *13,* 6183.

(13) (a) Nosaka, Y.; Yamaguchi, K.; Miyama, H.; Hayashi, H. *Chem. Lett.* **1988,** 605. (b) Fischer, C.-H.; Henglein, A. *J. Phys. Chem.* **1989,** *93,* 5578. (c) Rogach, A. L.; Kornowski, A.; Gao, M.; Eychmuller, A.; Weller, H. *J. Phys. Chem. B* **1999,** *103,* 3065. (d) Yang, C.-S.; Bley, R. A.; Kauzlarich, S. M.; Lee, H. W. H.; Delgado, G. R. *J. Am. Chem. Soc.* **1999,** *121,* 5191. (e) Ogawa, S.; Hu, K.; Fan, F.-R. F.; Bard, A. J. *J. Phys. Chem. B* **1997,** *101,* 5707. (f) Guo, L.; Ai, X. *Mater. Chem. Phys.* **2000,** *63,* 30.

interface or deposited onto solid substrates (using the Langmuir–Blodgett (LB) technique) as the interfacial stabilizers where nanoparticles are formed when the metal (counter-)cations at the polar head region are exposed to, for instance, an atmosphere of H_2S.[12] However, in the solid composite systems, it becomes technologically challenging when chemical or physical modifications of the nanoparticles are desired; whereas in the "naked" colloid systems, the particles typically lack long-term stability, especially when solvents are removed. Thus, some attempts have been reported to produce organic monolayer-protected semiconductor nanoparticles,[2,5,11,13] which, akin to the metal counterparts, demonstrate great stability in both solution and dry forms, and, more importantly, can be further decorated by surface exchange or coupling reactions by virtue of the functional moieties on the protecting monolayers. On the other hand, because surface chemical modifications play an important role in governing the particle surface energetic states of electrons and holes, this could provide a molecular framework to manipulate the nanoparticle electronic structures and hence macroscopic properties, reflected, for instance, in their optical absorption and photoluminescence measurements.[13]

Another intrinsic property related to semiconductor nanoparticles is their photochemical characteristics,[1] e.g., photoinduced charge transfer. These have been investigated for their potential applications in, for instance, solar energy conversion and photochemical reaction catalysis. Because the electronic energy distribution is dependent upon the specific molecular structure as well as physical dimension of the nanoparticles, the associated electron-transfer chemistry can be regulated at the molecular level.[1,13e] Among these, quite extensive research has been directed toward the understanding of the electrochemical behaviors of PbS semiconductors, either in bulk[14] or nanoparticle[13e] form. However, prior research has primarily focused on aqueous-phase electrochemistry, whereas little is known about the voltammetric responses in nonaqueous solvents. By passivating the PbS nanoparticles with hydrophobic alkanethiolates, the particles are rendered soluble in nonaqueous media, which will provide a glimpse of the solvent effect on their charge-transfer chemistry.

In this report, we first describe a solution-based approach to synthesize nanosized PbS particles passivated by a monolayer of alkanethiolates under ambient conditions, followed by the studies of the reaction dynamics of the particle formation, as well as the experimental control of the particle dimensions. Spectroscopic investigations that include UV–Vis and luminescence measurements are carried out, along with electrochemical measurements of their solution-phase electron-transfer properties.

Experimental Section

Chemicals. Lead acetate (Pb(Ac)$_2$, ACROS), palladium chloride (PdCl$_2$, ACROS), silver nitrate (AgNO$_3$, Fisher),

tetrachloroauric acid (HAuCl$_4$·xH$_2$O, Aldrich), sodium sulfide (Na$_2$S, Fisher), *1*-hexanethiol (C6SH, Aldrich, 96%), and tetra-*n*-butylammonium perchlorate (TBAP, ACROS) were all used as received. All solvents were obtained from typical commercial sources and used as received as well except for CH$_2$Cl$_2$ which was freshly distilled in the presence of P$_2$O$_5$ just prior to use. Water was supplied from a Barnstead Nanopure Water system (18.3 MΩ).

Particle Synthesis. Preparation of gold,[15] silver,[15b] and palladium[16] nanoparticles passivated by monolayers of *1*-hexanethiolates has been described previously. The average particle core size was 1.6, 2.7, and 2.5 nm, respectively, as determined by transmission electron microscopy (TEM).

For the synthesis of PbS nanoparticles, in a typical reaction, 1 mmol of Pb(Ac)$_2$ was dissolved in 50 mL of methanol and 2 mmol of C6SH was dissolved in 5 mL of methanol. The C6SH was then added slowly in a dropwise fashion into the Pb(Ac)$_2$ solution under vigorous stirring. The resulting solution became cloudy and the color turned yellow. Fifty milliliters of toluene was then added into the solution followed by 50 mL of Nanopure water. The toluene phase was then rinsed several times with Nanopure water and separated from the aqueous phase using a separatory funnel. To the toluene phase was then added 0.1 mmol of Na$_2$S that was dissolved in 5 mL of methanol, again, in a dropwise manner and under vigorous stirring. The solution became dark brown and transparent, indicating the formation of PbS nanoparticles that were capped with an alkanethiolate monolayer and very soluble in toluene. The solution was then stirred for about 1 h before the solution was phase-separated by adding 50 mL of Nanopure water. The toluene phase was collected and dried at reduced pressure. Excessive methanol and acetone were then used to rinse the obtained dark brown solid, and the particles were found to be soluble in apolar solvents, such as dichloromethane, hexane, and benzene, but not in polar solvents, such as alcohols, acetone, and water, akin to alkanethiolate-protected metal nanoparticles.[15,16] The particles synthesized under these particular experimental conditions were denoted as C6–PbS (2x) where 2x reflects the 2-fold molar excess of C6SH over Pb. Particles with varied C6SH/Pb ratios were also synthesized in a similar manner, such as (0.5x), (1x), (1.5x), and (4x), i.e., with an initial experimental feed ratio of Pb/RSH/Na$_2$S varied at 1:x:0.1 (here the ratio of Pb/Na$_2$S was fixed at 1:0.1; higher ratios of Na$_2$S appeared to lead to flocculation of the resulting particles, suggesting that the particle core size was more sensitive to the concentration of sulfide). It should be noted that the above synthetic protocol was performed under ambient conditions.

In the dynamic study, an aliquot of the toluene solution (in the presence of the water phase) was removed from the reaction vessel at various time intervals after the addition of Na$_2$S solution, and rinsed with copious Nanopure water before being dried at reduced pressure. The particles were then collected and purified in a similar manner.

The purity of the particles was then examined by using proton NMR spectroscopy (Varian 300) with concentrated solutions of particles dissolved in benzene-d_6. The lack of sharp features indicated the absence of free ligands and other impurities.

Spectroscopic Studies. Particle core size was measured with a Hitachi 7100 transmission electron microscope at 75 keV coupled with an energy dispersive X-ray (EDX) analyzer for elemental analysis. Selected area electron diffraction (SAED) was also carried out in the TEM chamber. The samples were prepared by casting a drop of the particle solution in hexane onto a 200-mesh Formvar-coated copper grid.

UV–Vis spectroscopic studies were performed with an ATI Unicam UV4 spectrometer using a 1-cm quartz cuvette with

(14) (a) Paul, R. L.; Nicol, M. J.; Diggle, J. W.; Saunders, A. P. *Electrochim. Acta* **1978**, *23*, 625. (b) Paul, R. L.; Nicol, M. J.; Diggle, J. W. *Electrochim. Acta* **1978**, *23*, 635. (c) Gardner, J. R.; Woods, R. *J. Electroanal. Chem.* **1979**, *100*, 447.

(15) (a) Templeton, A. C.; Wuelfing, W. P.; Murray, R. W. *Acc. Chem. Res.* **2000**, *33*, 27. (b) Whetten, R. L.; Shafigullin, M. N.; Khoury, J. T.; Schaaff, T. G.; Vezmar, I.; Alvarez, M. M.; Wilkinson, A. *Acc. Chem. Res.* **1999**, *32*, 397.

(16) Chen, S.; Huang, K.; Stearns, J. A. *Chem. Mater.* **2000**, *12*, 540.

a resolution of 2 nm. Luminescence studies were carried out with a Shimadzu RF-5301PC Spectrofluorophotometer. Both experiments were performed at ambient temperature. The particle solutions were typically 1–10 μM in CH_2Cl_2. In the quenching studies, the C6–PbS solution was diluted by the addition of a CH_2Cl_2 solution of *1*-hexanethiolate-protected transition-metal (vide ante) particles (15–30 μM), where excitation as well as emission spectra were collected.

Electrochemical Studies. Electrochemical measurements were performed with a BAS 100BW electrochemical workstation. A polycrystalline platinum disk electrode (sealed in a glass tubing; electrode area ca. 0.78 mm²) was used as the working electrode, a Ag/AgCl wire and a Pt coil were used as the reference and counter electrodes, respectively. The Pt working electrode was first polished with 0.05 μm Al_2O_3 slurries (Bruehler), and then sonicated in diluted HNO_3, H_2SO_4, and Nanopure water successively. Electrochemical etching of the Pt electrode was carried out briefly (~5 min) in 0.1 M H_2SO_4 by cycling the potentials between −0.5 and +0.6 V at 10 V/s. Particle solutions were prepared in freshly distilled CH_2Cl_2 with 0.1 M tetra-*n*-butylammonium perchlorate (TBAP) as the supporting electrolyte, which was deaerated with high-purity argon for at least 20 min prior to data acquisition and blanketed with an Ar atmosphere during the entire experimental process.

Results and Discussion

In this section, we first describe the synthesis of a series of PbS nanoparticles protected by *1*-hexanethiolate monolayers, with emphases on the reaction dynamics as well as experimental manipulations of the particle size and dispersity by using TEM. The optical and luminescence studies are then carried out to investigate the nanoparticle electronic energy structures, which are correlated to the particle dimensions estimated above, followed by solution-phase electrochemical studies of the particle charging properties at ambient temperature.

Reaction Dynamics of PbS Nanoclusters. TEM has been used rather extensively to measure the nanoparticle size in a direct and visual manner. For instance, previously, TEM has been used to investigate the growth dynamics of alkanethiolate-protected palladium[16] and gold[17] nanoparticle by measuring the temporal profiles of the particle dimensions. For "naked" semiconductor nanoparticles, it has been found that the overall particle size increases with time, most probably ascribed to the Ostwald ripening, where large particles grow even larger at the expense of the smaller ones, resulting in the fluctuation of particle size distributions as well.[5b] Therefore, it will be of fundamental importance to investigate the effects of protecting monolayers on the growth dynamics of the resulting particles, where, presumably, the particle size and size distribution will be less likely to fluctuate with time. Figure 1 shows the representative TEM micrographs of C6–PbS (**2***x*) particles acquired at various reaction times after the addition of Na_2S (A, 0.5 h; and B, 10 h), with insets showing the corresponding particle size histograms. One can see that the majority of the particles fall into the range of 2–4 nm in diameter with mostly spherical particle shape and around 30% size dispersity. The overall results are summarized in Figure 1C. Note that the particle size appears to vary only slightly within the
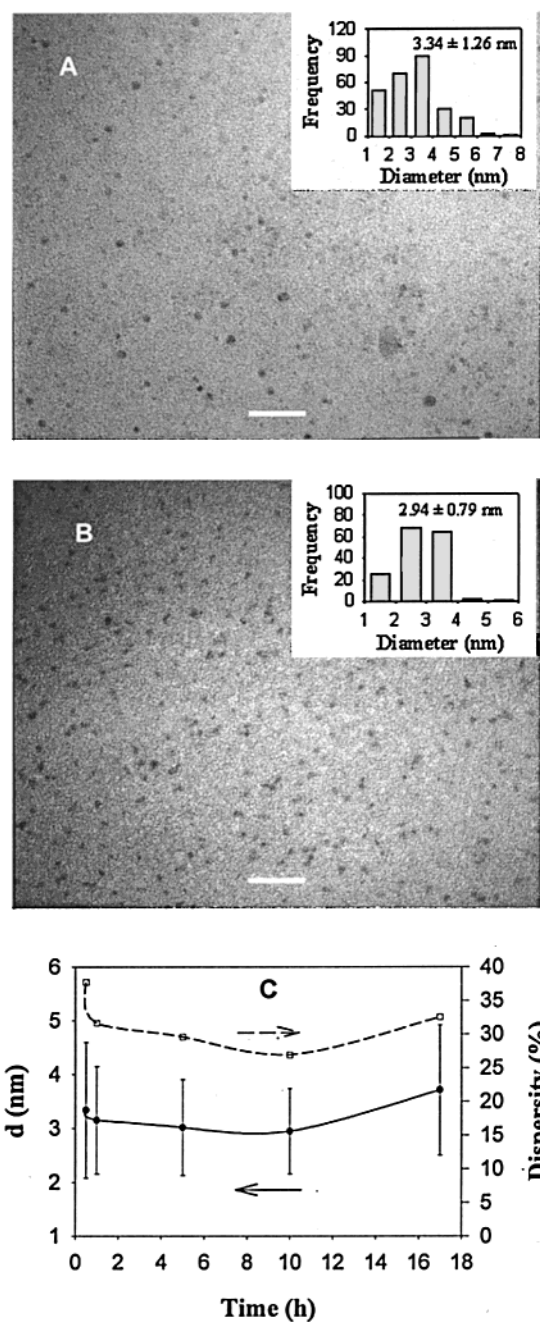
Figure 1. Representative TEM micrographs of C6–PbS (**2***x*) nanoparticles synthesized at various reaction times after the addition of Na_2S: (A) 0.5 h; and (B) 10 h. Scale bar 33 nm. Insets show the corresponding particle size histograms. (C) Variation of particle size and dispersity with reaction times.

experimental time range up to 17 h, with the smallest mean particle size and narrowest size dispersity found at about 10 h after the addition of Na_2S. These small variations of the particle size and size distribution indicate that the particles with the alkanethiolate protecting monolayers are rather stable even only 30 min after the reaction, in contrast to the "naked" colloidal systems.[5b] This might be attributed to the strong Pb–S bonding interactions involved in the particle core assembling as well as in the formation of alkanethiolate monolayers on the core surface.[18] This is consistent with earlier studies of the growth dynamics of alkanethiolate-protected gold[17] and palladium[16] nanoparticles, where very little fluctuation in particle size
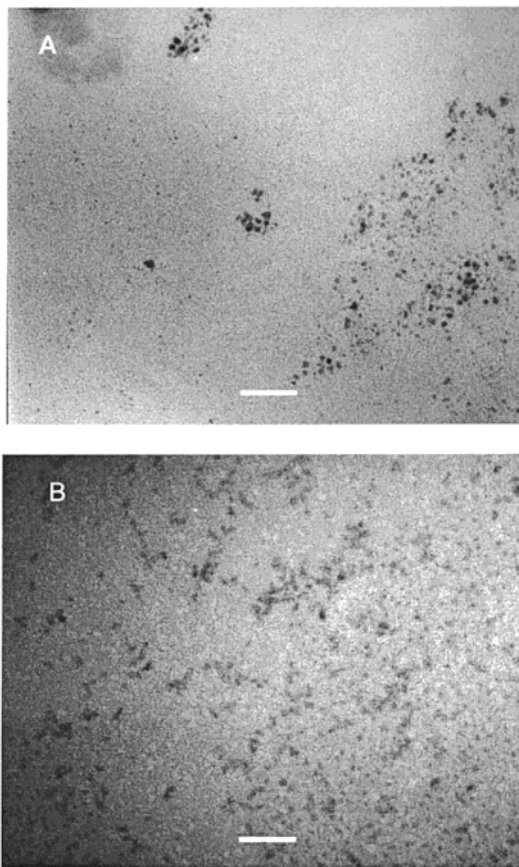
(17) Chen, S.; Templeton, A. C.; Murray, R. W. *Langmuir* **2000**, *16*, 3543.
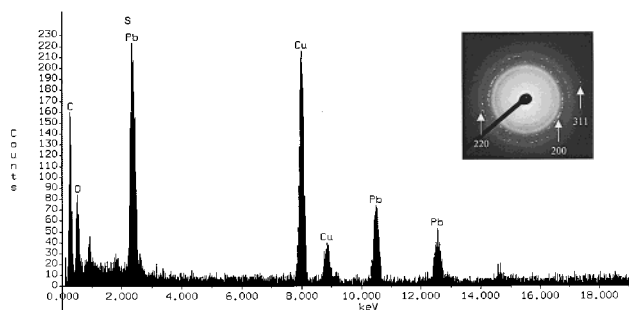
Figure 2. Energy dispersive *x*-ray analysis of the C6−PbS (2*x*) nanoparticles synthesized above at 1 h. Inset shows the corresponding selected area electron diffraction patterns. Rather consistent results were observed with other members of the PbS particle series synthesized here.

and dispersity was observed for the former; whereas for the latter, drastic variation was found.

The formation of PbS nanoparticles was further confirmed by EDX analysis (Figure 2), where the L_β, L_α, and M_α lines of Pb can be easily recognized at 12.650, 10.550, and 2.346 keV, respectively; whereas the S Kα line (2.307 keV) appears to be overlapped with the Pb Mα line (the appearance of Cu signals is attributed to the TEM grid). In addition, selected area electron diffraction (Figure 2 inset) shows a series of spotty fringes, indicating rather well-defined crystalline structure of the PbS particle materials, with the three brightest ones corresponding to the (200), (220), and (311) diffraction planes (PbS crystals are known to have a NaCl-like cubic structure with a lattice constant $a = 0.594$ nm).[3]

The above dynamic study demonstrates that the alkanethiolate-protected PbS particles are quite stable. Experimentally, typical reaction time was therefore set to 1−2 h. Here, we also carried out studies to explore the experimental control of the particle size and size dispersity by varying the feed ratios of the reactants. Figure 3 shows the representative TEM micrographs of a series of PbS−C6 particles synthesized with varied C6SH/Pb ratios (and fixed ratio of Pb/Na$_2$S = 1:0.1), from 0.5:1, to 1:1, 1.5:1, and 4:1 (denoted as 0.5*x*, 1*x*, 1.5*x*, and 4*x*, respectively), and the corresponding size and dispersity are summarized in Table 1. Note that the resulting particles show only a rather subtle variation of core size with the varied feed ratios of alkanethiol/lead. However, except for the 0.5*x* samples, the C6−PbS particles appear to decrease in size with increasing excess of alkanethiols, akin to the observations in the synthesis of alkanethiolate-protected gold[15] and CdS[13a,b] nanoparticles. Because in the formation of PbS nanocores, S^{2-} ions displaced the alkanethiolate ligands in the RS−Pb polymers and clustered the neighboring Pb ions forming the nanosized spherical structure, the more excess of the alkanethiols, the less likely that they will be replaced by the sulfide ions and hence smaller particles. The 0.5*x* sample appears to contradict this argument; however, it should be noted that the size measured only reflects the small portion of particles that are soluble, whereas most of the

(18) For instance, the bond strengths of Pb−S, Au−Au, and Pd−Pd are 346, 224.7, and 100 kJ/mol, respectively (Lide, D. R., Ed. *Handbook of Chemistry and Physics*, 76th ed.; CRC Press: Boca Raton, 1995).

Figure 3. Representative TEM micrographs of C6−PbS nanoparticles synthesized at various C6SH/Pb ratios: (A) 0.5*x*; and (B) 4*x* scale bar 33 nm. The overall results are summarized in Table 1.

collected solids appear to be aggregated and insoluble in most common solvents.

UV−Vis Spectroscopy. Nanosized semiconductor particles generally exhibit a threshold energy in the optical absorption measurements, due to the size-specific band gap structures,[1−8] which is reflected by the blue shifting of the absorption edge (from near-infrared to visible) with decreasing particle size.[1−13] This might provide an indirect way to evaluate, at least qualitatively, the variation of particle core dimensions.[3,8] Figure 4 shows the optical spectra of the series of C6−PbS nanoparticles that were synthesized with varied initial feed ratios of C6SH/Pb. One can see that for the relatively larger particles (1*x*−4*x*, Table 1), all show a rather similar and largely featureless absorption profile. In a previous study[11] with alkanethiolate-capped PbS nanoparticles synthesized in a bicontinuous cubic lipid matrix, it was reported that a broad absorption band was also observed at ca. 300 nm. In addition, for these particles (i.e., 1*x*−4*x*), the absorption edge is found at between 1.5 and 1.8 eV (700−800 nm).

In contrast, for the smaller particles (0.5*x*), molecular absorption features are quite dominant at $\lambda < 400$ nm with an additional broad absorption band at 460 nm, and an absorption edge quite clearly defined at a much shorter wavelength (560 nm or 2.2 eV), visibly demonstrating the quantum confinement effect.[1−8] These observations are in qualitative agreement with the above TEM measurements (Table 1). However, they are somewhat larger than the particle band gap calculated

Table 1. Variation of the Size and Dispersity of PbS Nanoparticles Protected by *1*-Hexanethiolate Monolayers at Different Synthetic Conditions

samples	0.5x	1x	1.5x	2x	4x
mean size (nm)	2.53 ± 1.15	3.98 ± 1.06	3.41 ± 1.36	3.61 ± 1.31	3.00 ± 1.15
dispersity	45.45%	26.63%	39.88%	36.29%	38.33%
no. of atoms[a]	346	1070	726	838	528

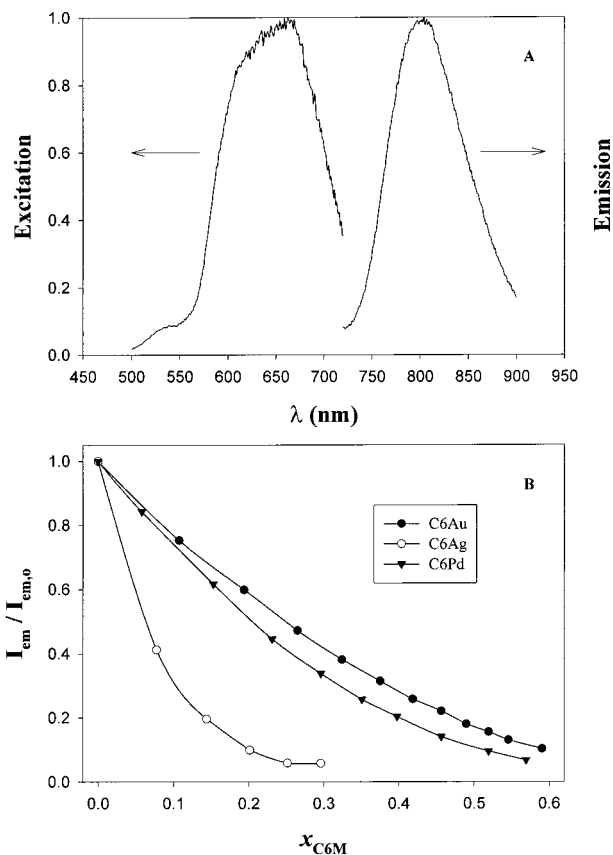[a] On the basis of the projection of spherical PbS nanoparticles.[8b]
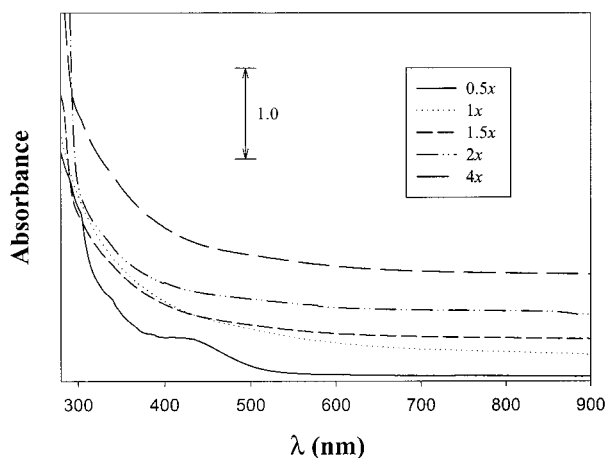
Figure 4. UV–Vis spectra of the C6–PbS particles synthesized under various conditions. The absorption spectra were offset for the sake of clarity. Particles were dissolved in CH_2Cl_2 with a concentration ca. 0.1 mg/mL.

on the basis of particle size.[8b] The discrepancy could be partly attributed to the underestimation of the particle core size because the very small ones might be overlooked due to poor background contrast in the TEM micrographs, as well as to the variation of chemical environment of the PbS nanoparticles, compared to earlier studies.[3,8]

Photoluminescence Spectroscopy. Another unique property associated with semiconductor nanoparticles is their luminescence characteristics, with the specific emission wavelengths dependent upon the nature of the semiconductors, the physical dimensions, as well as the chemical environments,[1,2,4] leading to great application potentialities in the fields of optoelectronic (light-emitting) devices[2] and biosensors.[5]

The fluorescence of PbS nanoparticles is generally rather weak, but detectable at the visible region.[19] For instance, a fluorescence peak at 700 nm was observed with PbS nanoparticles (1.5–2.5 nm in diameter) protected by poly(vinyl alcohol).[19a] Here the C6–PbS (1.5x) nanoparticle sample was taken as the illustrating example to investigate the luminescence properties by collecting the corresponding excitation as well as fluorescence spectra. Figure 5A shows the excitation (with emission wavelength λ_{em} set at 740) and emission (excitation wavelength λ_{ex} at 700 nm) spectra of the C6–PbS (1.5x) nanoparticles synthesized above in CH_2Cl_2 with a concentration of ca. 10 μM. The broad excitation band is probably composed of two overlapped bands centered at 610 and 665 nm, respectively, with an additional small shoulder at 536 nm; whereas in the emission spectrum, a rather sharp peak is observed at 804 nm (i.e., red fluorescence), which is ascribed to the

(19) (a) Gallardo, S.; Gutiérrez, M.; Henglein, A.; Janata, E. *Ber. Bunsen-Ges. Phys. Chem.* **1989**, *93*, 1080. (b) Machol, J. L.; Wise, F. W.; Patel, R.; Tanner, D. B. *Phys. A* **1994**, *207*, 427.


Figure 5. (A) Excitation and emission spectra of the C6–PbS (1.5x) nanoparticles in CH_2Cl_2. Excitation profile was acquired with emission wavelength (λ_{em}) set at 740 nm, whereas for the emission spectrum, the excitation wavelength (λ_{ex}) was set at 700 nm. These two spectra were normalized to their respective maximum intensity at 665 and 804 nm. (B) Variation of the PbS photoluminescence peak (804 nm) intensity where the C6–PbS solution was diluted by the addition of a CH_2Cl_2 solution of *1*-hexanethiolate-protected nanoparticles of gold, silver, or palladium. x_{C6M} (M = Au, Ag, and Pd) denotes the molar fraction of metal particles in the PbS solution. The original concentrations for the C6–PbS, C6Au, C6Ag, and C6Pd particles were 10, 30, 30, and 15 μM, respectively. The peak intensities were normalized to those prior to dilution. Lines are for eye-guiding only.

so-called band edge luminescence (BEL).[19] The red shift of the fluorescence peak, as compared to the literature results,[19a] is consistent with the larger particle core size.

In addition, as transition-metal nanoparticles exhibit strong absorption in the visible range,[15b,16] it might be interesting to study their quenching effects on the photoluminescence of semiconductor particles. It has been rather well known that nanosized transition-metal particles exhibit a UV–Vis absorption profile that decays exponentially with decreasing photon energy (the so-called Mie scattering), and, depending on the specific elements of the metal cores, might also feature a surface-plasmon (SP) absorption band. For instance, the SP bands of gold and silver nanoparticles can be found

at around 520 and 430 nm,[15] respectively, whereas Pd nanoparticles do not have any well-defined SP band.[16]

As a preliminary attempt, we used a binary mixture of the metal and PbS semiconductor nanoparticles in solution and measured the corresponding fluorescence responses. Figure 5B depicts the variation of the peak intensity (804 nm) of the PbS photoluminescence with the concentration of added metal nanoparticles (C6Au, C6Ag, and C6Pd). Upon the introduction of the metal nanoparticles into the PbS solution, the photoluminescence of PbS particles decreases rather significantly. For instance, when the molar ratio of metal particles vs PbS particles in solution reached 1:1 (i.e., $x_{C6M} = 0.5$ with M = Au, Ag, and Pd), at least 80% of the original intensity of the PbS luminescence was lost; and at higher concentrations of metal particles, the luminescence signal was barely detectable. This drastic decrease of the luminescence intensity of PbS particles could not be accounted for by the decrease of the PbS concentration alone. In fact, dilution of the PbS solution with CH_2Cl_2 alone led to only a very subtle change of the luminescence intensity. Instead, it is more likely due to the absorption of metal particles at the excitation and emission wavelengths, despite their relatively low absorption at the red end. This is consistent with the observation that the quenching efficiency increases in the order of Ag > Pd > Au (Figure 5B), which might be partly interpreted by the decreasing order of the particle core size (see the Experimental Section), because the absorption (Mie scattering) intensity at the long-wavelength region is more sensitive to the particle physical dimensions than to the specific elements of the particle core metals.[15b] Murray et al. also observed similar behaviors when gold nanoparticles and dansyl cadaverine were co-dissolved in solution;[20] however, it should be noted that the emission maximum of dansyl cadaverine (498 nm) is close to the SP band of gold particles.

Another possible interpretation is that the PbS luminescence is quenched by interparticle energy transfer. However, fluorescence quenching is distance-dependent[21] and in the present case, the two types of particles had no physical attachment in solution. In addition, on the basis of the particle concentrations in solutions, the particles were separated in an effective distance at least 1 order of magnitude of their size. Thus, it is highly unlikely that interparticle energy transfer played a significant role here.
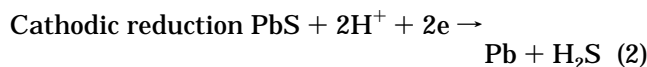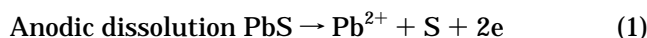
More detailed studies are desired to further investigate the effect of the particle core metals and sizes on their quenching properties. This might be exploited to chemically regulate the photoluminescence properties of semiconductor particles, especially in solid thin-films.

Electrochemical Studies. Earlier electrochemical studies of PbS were mainly focused on the anodic dissolution of bulk galena (main component PbS) for the extraction of lead metal,[14] as well as on the photoinduced charge transfer[13e] involving nanosized PbS particles for photochemical applications. It should be noted that these studies of PbS nanoparticles, as well as those of bulk PbS, were carried out in *aqueous* media, where
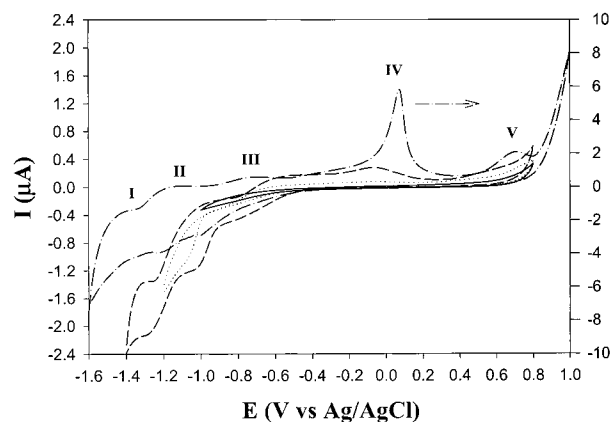
Figure 6. Cyclic voltammograms of a Pt electrode (0.78 mm²) in C6−PbS (4*x*) nanoparticles (ca. 0.4 mM) dissolved in freshly distilled CH_2Cl_2 containing 0.10 M tetra-*n*-butylammonium perchlorate (TBAP) within varied potential windows. The potential sweeps were always started cathodically, and the potential sweep rate 100 mV/s.

the reaction mechanism was proposed as

$$\text{Anodic dissolution } PbS \rightarrow Pb^{2+} + S + 2e \tag{1}$$

$$\text{Cathodic reduction } PbS + 2H^+ + 2e \rightarrow Pb + H_2S \tag{2}$$

and could be complicated by solution pH.[14] However, the electrochemical behaviors of PbS quantum dots in nonaqueous media remained largely unexplored, primarily because of the lack of hydrophobic PbS particles. The passivation of the PbS nanoparticles by alkanethiolate monolayers, as described above, renders the resulting particles soluble in nonaqueous media, providing a molecular system where the media effect on the electrochemical processes can then be investigated.

Figure 6 shows the cyclic voltammogram of the C6−PbS (4*x*) nanoparticles dissolved in freshly distilled CH_2Cl_2 containing 0.10 M TBAP. The potential sweeps were started at 0 and initially went in the cathodic direction. One can see that within the potential regime of −1.0 to +0.8 V (─), only featureless voltammetric currents are exhibited. This "flat" region might partly arise from the band gap[22a] of these nanosized PbS particle molecules, and appears to be consistent with the aforementioned UV−Vis and TEM results (1.5−1.8 eV). When the negative potential is expanded to −1.2 V (···), a pair of voltammetric waves appear at −1.0 V with no other well-defined voltammetric features in the rest of the potential window. When the potential is expanded further in the negative direction (−1.4 V, - - -), three pairs of rather well-defined waves can be found (labeled I, II, and III) at −1.3, −1.0, and −0.67 V, respectively (an additional anodic wave was observed at −0.07 V with no apparent return wave; more discussions below).

These three waves show a modest peak splitting (ranging from 20 to 200 mV), suggesting quasi-reversible electron-transfer processes; and the peak potential spacing is almost constant at about 300 mV. At first

(20) Aguila, A.; Murray, R. W. *Langmuir* **2000**, *16*, 5949.
(21) Zelent, B.; Kusba, J.; Gryczynski, I.; Johnson, M. L.; Lakowicz, J. R. *J. Phys. Chem.* **1996**, *100*, 18592.

(22) (a) Chen, S.; Ingram, R. S.; Hostetler, M. J.; Pietron, J. J.; Murray, R. W.; Schaaff, T. G.; Khoury, J. T.; Alvarez, M. M.; Whetten, R. L. *Science* **1998**, *280*, 2098. (b) Chen, S.; Murray, R. W.; Feldberg, S. W. *J. Phys. Chem. B* **1998**, *102*, 9898.

glance, this appears to be consistent with the so-called electrochemical quantized capacitance charging to monolayer-protected nanoparticles,[22] where the particle molecules behave as diffusive nanoelectrodes in solution and the discrete charging to the particle double-layer results in the appearance of electrochemical analogues of Coulomb staircase charging.[22]

However, if these voltammetric waves are indeed due to the single-electron quantized charging to the PbS nanoparticle double layers, the corresponding molecular capacitance (C_{MPC}) evaluated from the peak spacing (ΔV), $C_{MPC} = e/\Delta V$, where e is the electronic charge, is ca. 0.5 aF, about three times smaller than that predicted from the physical dimension of the particle.[22b] In fact, it is more likely that these voltammetric features are due to the cathodic reduction reactions of the PbS nanocrystals,[14] as further supported by the voltammetric responses at an even wider potential window ($-\cdot-$), -1.6 to $+1.0$ V. One can see that, in addition to the three pairs of voltammetric waves observed in the negative potential region, there are two rather well-defined anodic wave observed at $+0.1$ and $+0.7$ V, respectively (labeled IV and V). In particular, peak IV becomes rather prominent, compared to that observed in the previous potential window (-1.4 to $+0.8$ V, - - -). Whereas the detailed reaction mechanism remains largely unknown at the moment, it is most likely that the voltammetric waves (I, II, and III) are related to the reductive decomposition of PbS and Pb$-$SC6 to lead and the corresponding sulfur or thiolate (here it is unlikely that reaction 2 was followed because freshly distilled solvent was used). The sharp feature of peak IV (at 0.1 V) might reflect the anodic stripping of surface accumulation of lead. The peak (IV) height became more pronounced at slower potential sweep rate and the peak position shifted anodically at increasing sweep rate, indicating a kinetically sluggish process. Peak V and the sharply rising anodic current at even more positive potentials might be ascribed to the anodic dissolution of PbS (reaction 1).[14] These faradaic processes gave rise to a rather significant increase of the overall voltammetric currents (Figure 6). One might note that, as compared to the observations in *aqueous* media,[14] the voltammetric responses described here in organic (CH$_2$Cl$_2$) solution show a rather significant overpotential in the cathodic as well as the anodic processes, indicating that the monolayer-protected PbS nanoparticles are more stable in hydrophobic media. More detailed studies are desired to address the reaction mechanism and the associated solvent effects.

Concluding Remarks

Alkanethiolate-protected PbS nanoparticles were synthesized using a solution chemistry method. The particles exhibited great stability during particle growth and only varied slightly with different initial feed ratios of lead and alkanethiol. The particle band gap structures, as determined by UV$-$Vis measurements, were found to be consistent with their physical dimensions. The photoluminescence intensity of the PbS particles was found to be depressed greatly by the presence of transition-metal nanoclusters, presumably due to the absorption of metal particles at the excitation and emission wavelengths. Electrochemical studies revealed three pairs of rather well-defined and quasi-reversible voltammetric waves in the negative potential regime (-0.6 to -1.6 V), which are most likely attributed to the cathodic reduction of PbS; whereas anodic dissolution was observed at potentials more positive than 0.7 V. These observations indicate that there is a rather large overpotential associated with the faradaic processes of PbS in organic media, as compared to those in aqueous solution.[14]

CM000653E